Received: 15 January 2019 | Revised: 22 May 2019 | Accepted: 22 May 2019

DOI: 10.1111/ejn.14477

RESEARCH REPORT

EJN European Journal of Neuroscience FENS WILEY

# Involvement of rat posterior prelimbic and cingulate area 2 in vocalization control

**Peter Julian Garnett Bennett**[1,2] | **Eduard Maier**[1] | **Michael Brecht**[1,2,3]

[1]Bernstein Center for Computational Neuroscience Berlin, Humboldt-Universität zu Berlin, Berlin, Germany

[2]German Center for Neurodegenerative Diseases, Berlin, Germany

[3]NeuroCure Cluster of Excellence, Humboldt-Universität zu Berlin, Berlin, Germany

**Correspondence**
Michael Brecht, Bernstein Center for Computational Neuroscience Berlin, Humboldt-Universität zu Berlin, Philippstr. 13, House 6 Berlin, Germany.
Email: michael.brecht@bccn-berlin.de

**Funding information**
Deutsche Forschungsgemeinschaft; Deutsches Zentrum für Neurodegenerative Erkrankungen

**Abstract**

Microstimulation mapping identified vocalization areas in primate anterior cingulate cortex. Rat anterior cingulate and medial prefrontal areas have also been intensely investigated, but we do not know, how these cortical areas contribute to vocalizations and no systematic mapping of stimulation-evoked vocalizations has been performed. To address this question, we mapped microstimulation-evoked (ultrasonic) vocalizations in rat cingulate and medial prefrontal cortex. The incidence of evoked vocalizations differed markedly between frontal cortical areas. Vocalizations were most often evoked in posterior prelimbic cortex and cingulate area 2, whereas vocalizations were rarely evoked in dorsal areas (vibrissa motor cortex, secondary motor cortex and cingulate area 1) and anterior areas (anterior prelimbic, medial-/ventral-orbital cortex). Vocalizations were observed at intermediate frequencies in ventro-medial areas (infralimbic and dorsopeduncular cortex). Various complete, naturally occurring calls could be elicited. In prelimbic cortex superficial layer microstimulation evoked mainly fear calls with low efficacy, whereas deep layer microstimulation evoked mainly 50 kHz calls with high efficacy. Vocalization stimulation thresholds were substantial (70–500 μA, the maximum tested; on average ~400 μA) and latencies were long (median 175 ms). Posterior prelimbic cortex projected to numerous targets and innervated brainstem vocalization centers such as the intermediate reticular formation and the nucleus retroambiguus disynaptically via the periaqueductal gray. Anatomical position, stimulation effects and projection targets of posterior prelimbic

**Abbreviations:** 4v, Fourth ventricle; 7n, Facial nerve; AAV, Adeno-associated virus; antPrL, Anterior prelimbic cortex; BDA, Biotinylated dextran amine; Cg1, Cingulate area 1; dlPAG, Dorsolateral periaqueductal gray; Flex, Flipped extension; DPC, Dorsopeduncular cortex; GFP, Green fluorescent protein; InL, Infralimbic cortex; IRT, Intermediate reticular nucleus; lPAG, Lateral periaqueductal gray; LRt, Lateral reticular nucleus; M1, Primary motor cortex; M2, Secondary motor cortex; MdD, Medullary reticular nucleus, dorsal part; MdV, Medullary reticular nucleus, ventral part; MO, Medial-orbital area; NRA, Nucleus retroambiguus; PAG, Periaqueductal gray; PC-RtA, Parvocellular reticular formation, alpha part; Pr5VL, principal sensory trigeminal nucleus, ventrolateral part; PrL, Prelimbic cortex; postPrL, Posterior prelimbic cortex; RFP, Red fluorescent protein; Rt, Reticular formation.; vlPAG, ventrolateral periaqueductal gray; VMC, Vibrissa motor cortex; VO, Ventral-orbital area.

Peter Julian Garnett Bennett and Eduard Maier contributed equally to this work.

Edited by Thomas Klausberger.

cortex were similar to that of monkey anterior cingulate vocalization cortex. Our data suggest that posterior prelimbic cortex is more closely involved in control of vocalization initiation than in specifying acoustic details of vocalizations.

**KEYWORDS**

microstimulation, periaqueductal gray, prefrontal cortex, transsynaptic tracing, USVs

## 1 | INTRODUCTION

A series of now classic studies in monkeys (Hughes & Mazurowski, 1962; Jürgens & Ploog, 1970; Smith, 1945) identified cortical vocalization areas in anterior cingulate cortex in the last century. Electric stimulation of these areas evokes species-specific vocalizations both in monkeys (Jürgens & Ploog, 1970; Paus, 2001) and in humans (Sperli, Spinelli, Pollo, & Seeck, 2006). Interference with their function impairs vocalization control in monkeys (Aitken, 1981; Kirzinger & Jürgens, 1982) and leads to a loss of voice volume in humans (Jürgens & von Cramon, 1982). Non-human primate anterior cingulate cortex projects heavily to the periaqueductal gray (Müller-Preuss & Jürgens, 1976) and this pathway is thought to be critically involved in vocalization control (Jürgens, 1994, 2002).

In rats, medial prefrontal cortex/anterior cingulate cortex has been intensely studied as an area presumed to be involved in high-level executive control. Vocalization control by rat medial prefrontal cortex/anterior cingulate cortex has been looked at less, however. In fact, out of the more than 1,000 papers returned by a PubMed search for rat prelimbic cortex only one abstract mentions vocalizations in passing and there is no systematic vocalization mapping study by microstimulation in rats. We think our ignorance about cortical vocalization control in rats is almost certainly related to the fact that rats vocalize primarily in ultrasonic range, which makes it more difficult to study these vocalizations. Addressing the mechanisms of vocalization control in rats is important, because rats are extremely vocal animals. Thus, in their own interactions (Rao, Mielke, Bobrov, & Brecht, 2014) and in human–rat interactions (Ishiyama & Brecht, 2016; Panksepp & Burgdorf, 2003), rats vocalize at a high rate (on the order of 1 call per s per animal) and emit a wide variety of calls.

The rat prefrontal cortex consists of multiple areas (Öngür & Price, 2000). Its dorsal parts are occupied by primary vibrissa motor cortex and secondary motor cortex (Brecht et al., 2004). The anterior pole of medial prefrontal cortex is occupied by prelimbic and ventral and medial-orbital cortex. Dorsally and ventrally following cortical areas had been distinguished: cingulate area 1, cingulate area 2, infralimbic and dorsopeduncular cortex. There is scattered evidence suggesting that rodent medial prefrontal cortex might indeed contribute to vocalization control. Thus, in stimulation studies in rat prefrontal cortex calls were occasionally observed (Burgdorf, Wood, Kroes, Moskal, & Panksepp, 2007). Frysztak and Neafsey provided lesion evidence for an involvement of infralimbic cortex in the control of alarm calls emitted in an aversive conditioning paradigm (Frysztak & Neafsey, 1991). Recently, the vocal abilities of rodents found more attention both as indices of emotional processing (Knutson, Burgdorf, & Panksepp, 2002; Wöhr & Schwarting, 2013) and in the context of courtship (Arriaga, Zhou, & Jarvis, 2012) and microstimulation work in anesthetized guinea pigs observed vocalizations evoked from medial prefrontal areas (Green et al., 2018).

We applied systematic microstimulation mapping in awake head-fixed rats to chart electrically evoked vocalizations in areas of rat prefrontal cortex. To this end, we first determined if vocalizations could be electrically evoked by microstimulation in rat prefrontal cortex. After such stimulation mapping, we assessed how vocalization sites map onto areal boundaries of rat prefrontal cortex. We also assessed the characteristics of stimulation-evoked vocalizations. Finally, we probed the anatomical connections that might mediate vocalization by anterograde and transsynaptic tracing techniques.

## 2 | MATERIAL AND METHODS

### 2.1 | Animal welfare

All experimental procedures were performed according to German animal welfare law under the supervision of local ethics committees (Permit no. G279/18 and G0193/14). Male Long-Evans rats were purchased from Janvier (Genest-Saint-Isle, France). Implanted animals were housed in single animal cages, but were in visual, olfactory and auditory contact with other rats. All animals were kept on a 12 hr:12 hr reversed light/dark cycle with lights off at 8:00 a.m., so that all experiments were performed in the rats' dark phase. Rats had ad libitum access to food and water.

### 2.2 | Surgical and behavioral procedures for experiments with head-fixed animals

In these experiments, rats were between 4 and 8 weeks old. We used male Long-Evans rats that were handled for 2–3 days, before being implanted with a head-fixation post and a chamber over the medial frontal cortex. Before

surgery, the rats were briefly anesthetized with isoflurane and then injected i.p. with a dose of 100 mg/kg ketamine and 7.5 mg/kg xylazine. During the surgery, the anesthesia depth was monitored by watching the rat respiration rate, testing the pinch reflex and monitoring whisker micromovements. If the rat appeared to be entering a lighter state of anesthesia, additional alternating doses of 25% of the initial dose in ketamine/xylazine amount or 25% of the corresponding ketamine dose alone were given. Typically, this was needed about 1 hr after the first injection. During the surgery, the rat was placed on a heating pad and was kept at approximately 35°C using a feedback system attached to a rectal temperature probe (Stoelting). Ten minutes before the first incision, the scalp was locally anesthetized by injection of a 1% lidocaine solution. Then the rat was placed in a stereotaxic frame, the scalp was cut and the tissue on the skull removed. The chamber was cylindrical with a diameter of 4–6 mm and centered 2.5 mm anterior, 0.7 mm lateral from bregma. Most experiments targeted the left hemisphere. The surgery procedure including anesthesia and preparation of the skull was the same as described above. The head-fixation post and recording chamber were fixed to the skull using UV-curable adhesive (Kerr) and dental cement (Heraeus). After the first surgery, animals were given 2 days of rest and then habituated to head-fixation over several days. The rat was first head-fixed for 5 min in the first head-fixation session, then for an additional 10 min with each succeeding session until the rat was comfortable with head-fixation for 60 min. During the habituation procedure, the rat was also accustomed to the experimental setup (e.g. microscope light turning on and off, noise from the micromanipulator). Habituation to head-fixation took 2–4 days on average, depending on the rat's behavior. The preparation was covered with silicone (Kwik-Cast, World Precision Instruments) and additionally protected by a lid closing the cylinder.

## 2.3 | Microstimulation procedures

After animals were surgically prepared and habituated to head-fixation as described above, we inserted tungsten microelectrodes (Microprobes) into the brain through the intact dura. For microstimulation, we applied 0.3 ms unipolar negative-tip current pulses at 100 Hz at current intensities varying 10–500 μA. To determine current threshold for vocalization, current intensities were varied in 10 μA steps below 100 μA, in 50 μA steps between 100 and 200 μA and in 100 μA steps above thresholds of 200 μA. The minimal current that evoked vocalizations in 50% of cases was considered to be the threshold current. Current pulses were delivered from a stimulus isolator (World Precision Instruments), gated by TTL pulses sent from a custom build pulse-generator based on a microprocessor, model Arduino Uno. The stimulation paradigm was blocks of 1-s long stimulation trains (100 Hz, 300 μs pulse width) with 5 s pause intervals. Tracks of interest were labeled with electrolytic lesions by applying a direct current (8 s, 8 μA, electrode tip negative). At the end of experiments, animals received an overdose of the anesthetic and were transcardially perfused with a pre-fixative (0.9% NaCl, 0.02 M phosphate buffer) solution followed by a 4% paraformaldehyde solution and the brain was histologically processed. The above mentioned procedures were conducted in five animals. Tracks were assigned to cortical areas in four animals, as histological assignment of all tracks was not possible in one animal. Areal boundaries were drawn according to Paxinos & Watson, 1986 and Brecht et al., 2004 and the maps were analyzed in four animals. For testing whether the probability to evoke calls is different between layers, we performed surgery and habituation of rats as described above and inserted electrodes in prelimbic cortex of three rats at the following coordinates: 3 mm rostral from Bregma and at four lateral positions: 250, 500, 750 and 1,000 μm lateral from Bregma. At each lateral position, the electrode was lowered to the following stimulation sites: 1,500, 2,000, 2,500, 3,000, 3,500 and 4,000 μm depth. Stimulation parameters and histological preparation were as described above.

## 2.4 | Ultrasonic vocalization recording and analysis

Ultrasonic vocalizations (USVs) produced by the rats were recorded by a microphone positioned in front of the animal. For microphones, we used condenser ultrasound CM16/CMPA (frequency range 10–150 kHz) ultrasound microphones by Knowles. Data were acquired at a sampling rate of 250 kHz and 16-bit resolution using the Avisoft UltraSoundGate 416H and Avisoft-RECORDER software. USVs were visually identified and categorized using Audacity 2.1.2. Categorization followed Ishiyama and Brecht (2016). We compared electrically evoked calls to natural calls observed in rat tickling (Ishiyama & Brecht, 2016) and calls observed in rat facial interactions (Rao et al., 2014).

## 2.5 | Anterograde tracing

Solutions containing anterograde Biotinylated Dextrane Amine (BDA; 10% w/v dissolved in distilled water; 10.000 Molecular Weight) were injected in two male Long-Evans rats. Surgical procedures were the same as described above. Prior to tracer injection, we confirmed that microstimulation evoked calls, at the site targeted for injection (3 mm anterior from Bregma, 0.75 mm lateral from Bregma and at 3–4 mm depth). Glass electrodes with a tip diameter of

10–20 μm were filled with a 10% BDA solution and lowered into the target region at a depth of 3 mm below the pia. The tracer was iontophoretically injected using a stimulus isolator (National Instruments; 5 s on/off current pulses of 5–15 μA for 15 min). After the injections, the pipettes were left in place for several minutes and were then quickly retracted. The craniotomy was closed using silicone (Kwik-Cast) and dental cement (Heraeus). The animals were kept alive for 7 days to allow neuronal transport of BDA. Subsequently the animals were transcardially perfused with a pre-fixative solution (0.9% NaCl, 0.02 M phosphate buffer) followed by a 4% formaldehyde solution and the brain was histologically processed similarly as described below. For anterograde tracing, BDA containing neuronal projections were visualized by the reaction of diaminobenzidine with a biotin-binding streptavidin–peroxidase complex leading to brown precipitation (Vectastain ABC-Kit, Biozol); sections were mounted with Moviol (Roth). Brains were counterstained for cytochrome oxidase activity as described in Brecht and Sakmann (2002).

## 2.6 | Viral anterograde transsynaptic tracing

The anterograde transsynaptic tracing procedure was adapted from Zingg et al. (2016) and was applied in two rats. The logic of this transsynaptic labeling approach is that presynaptic neurons (in our case situated in the prelimbic area) are infected with a high titer adeno-associated virus 2/1 (AAV2/1) virus leading to the expression of Cre-recombinase and a nuclear fluorescent reporter. A smaller fraction of viral particles is then transsynaptically transported and induced the expression of Cre-recombinase and the fluorescent reporter in postsynaptic neurons (in our case neurons in the periaqueductal gray). As only a small fraction of viral particles are transsynaptically transported, it might not be possible to visualize the fluorescent reporter in postsynaptic cells due to low expression levels. However the high enzymatic efficacy of Cre-recombinase allows visualization of postsynaptic cells when infected by a virus that leads to Cre-dependent expression of another fluorescent reporter (in our case cytosolic green fluorescent protein (GFP)). This transsynaptic labeling procedure was carried out as follows: First, a Cre-expressing AAV1 virus (AAV1.Syn.iCre.RFP; $1.55 \times 10^{13}$ genome copies/ml; Viral Core Facility Charité, Berlin) was pressure injected in the prelimbic cortex (3 mm anterior, 0.7 mm lateral from Bregma, depth: 3 mm; 70 nl total quantity, 30 nl/min). For this, glass electrodes with a tip diameter of 10–20 μm were sequentially backfilled with ~5 μl virus-containing solutions and ~1 μl mineral oil (Sigma-Aldrich). Note that high titer is essential for the success of anterograde spread. General surgical procedures were the same as described above, except that additionally the dura was removed. Backfilled pipettes were placed into a stereotactic injector (Stoelting, Wood Dale, USA) and were slowly inserted into the brain. When the desired depth was reached, the injection was carried out after a 5 min waiting period and was followed by a 20 min waiting period. Successful injection was confirmed by the visualization of movement of the plunger relative to the pipette shaft during the injection. The pipette was then slowly retracted, the craniotomy was covered with Kwik-Cast silicone and the skin was sutured. Animals received 5 mg carprofen i.p. before waking up. Three days later a Cre-dependent GFP-flip-extension (flex) AAV1 virus (AAV1.CAG.flex.GFP; $1.42 \times 10^{12}$ genome copies/ml; Viral Core Facility Charité, Berlin) was injected in the periaqueductal gray (6.7 mm posterior and 0.7 mm lateral from Bregma, depth: 5 mm; 300 nl total quantity, 50 nl/min) the same way as described for the first injection. The two viral injections were done sequentially to allow clearance of the AAV1.Syn.iCre.RFP which is to prevent potential contamination of other areas by the spread of virus along the pia. Three weeks later animals were killed with an overdose of isoflurane and were transcardially perfused with 4% paraformaldehyde solution. The brain was removed from the skull and stored in 4% paraformaldehyde overnight. The brain was embedded in coagulated egg yolk (8 ml egg yolk, 1.3 ml PB and 1 ml Glutaraldehyde) to stabilize such that 80 μm coronal sections could be continuously cut on a vibratome (Mikrom HM 650 V, Thermo Scientific). Sections were coverslipped with mounting medium (Fluoromount, Biozol) and pictures were taken on a Leica DM5500B microscope (Wetzlar, Germany).

## 2.7 | Overview of mapping data

We habituated five rats to head-fixation and then systematically mapped their prefrontal cortices by microstimulation pulses applied through tungsten microelectrodes. We placed electrolytic lesions (10 s, 10 μA, direct current electrode tip negative) in each track and at the conclusion of the experiments, killed the animals by an overdose of the anesthetic. After transcardial perfusion, we recovered the brains for histological analysis. The spatial distribution of microstimulation effects was qualitatively similar in all five animals. In one animal, however, our attempts for histological reconstruction of microstimulation tracks failed and we therefore restricted the full analysis of results to four brains, in which we obtained complete histological verification of all stimulation sites.

# 3 | RESULTS

## 3.1 | Vocalizations evoked by microstimulation

Data from a representative microstimulation track are shown in Figure 1a. The micrograph shows a coronal brain section

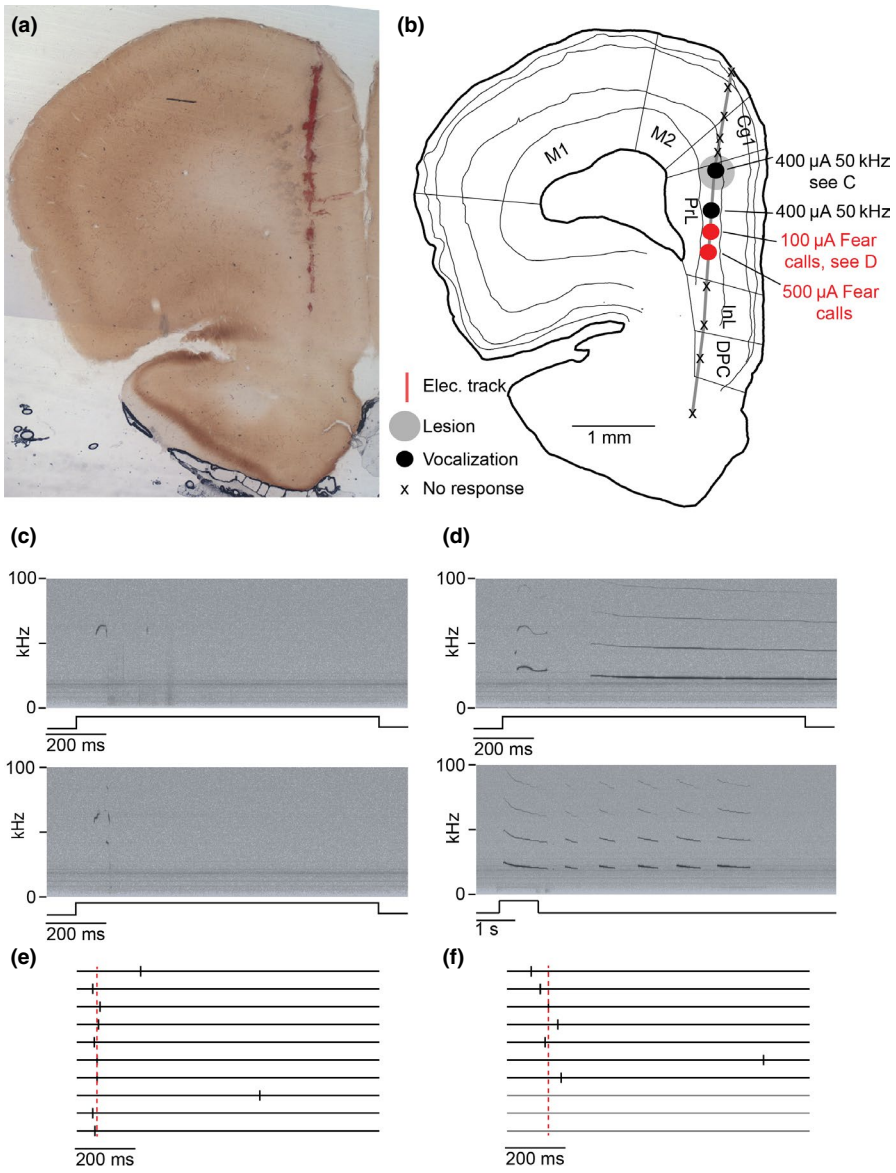


**FIGURE 1** Ultrasonic vocalizations evoked in a microstimulation penetration through rat frontal cortex. (a) Histological example of an electrode track and lesion in a cytochrome c oxidase-stained section cut in the coronal plane. (b) Schematic showing cortical areas along the path of the stimulation electrode. The gray line indicates the electrode track, whereas the gray circle indicates an electrolytic lesion. Microstimulations at sites marked by an x did not evoke vocalizations. Stimulations at sites marked by dots evoked vocalizations. The stimulation threshold and evoked call type are indicated for each individual site. Abbreviations: M1, primary motor cortex; M2, secondary motor cortex; Cg1, primary cingulate cortex; PrL, prelimbic cortex; InL, infralimbic cortex; DPC, dorsopeduncular cortex. (c) Top: Spectrogram of an example frequency-modulated 50 kHz vocalization, evoked by microstimulation in dorsal prelimbic cortex. Bottom: Spectrogram of an example frequency-modulated 50 kHz vocalization, comprising two components (~70 kHz & ~40 kHz), evoked by microstimulation in dorsal prelimbic cortex. (d) Top: Spectrogram of an example fear vocalization (or 22 kHz vocalization) including an initial frequency-modulated component and several harmonic components, evoked by microstimulation in ventral prelimbic cortex. Bottom: Spectrogram of an example fear vocalization (or 22 kHz vocalization) including several harmonic components, evoked by microstimulation in ventral prelimbic cortex. Note the different time scale. (e) Plot showing onset latencies for 50 kHz vocalizations upon microstimulations in prelimbic cortex across 10 trials. Line plots are aligned to stimulation onsets as indicated in C. Red dashed line indicates median latency at 67 ms. (f) Plot showing onset latencies for fear vocalizations upon microstimulations in prelimbic cortex across ten trials. Red-dashed line indicates median latency at 137 ms. Line plots are aligned to stimulation onsets as indicated in D. Gray lines indicate trials that did not evoke vocalizations. [Colour figure can be viewed at wileyonlinelibrary.com]

stained for cytochrome oxidase activity. The track is clearly visible and a drawing of the track, the stimulation sites and cortical area boundaries are shown in Figure 1b. In this track, we observed a sequence of nonresponsive sites (marked with an x) dorsally (in secondary motor cortex and cingulate area 1) followed ventrally by sites in prelimbic cortex, at which we observed electrically evoked vocalizations (marked with black dots), followed ventrally again by unresponsive sites

in infralimbic and dorsopeduncular cortex (Figure 1b). Spectrograms of microstimulation-evoked 50 kHz vocalizations are shown in Figure 1c and spectrograms of microstimulation-evoked fear calls are shown in Figure 1d. Calls could be assigned with great certainty as electrically evoked, because the rate of spontaneous vocalizations was extremely low in most experiments, that is, spontaneous vocalizations were often entirely absent. Calls could also outlast the electric stimulation for several seconds (Figure 1d). The raster schematics of onset latencies for the 50 kHz vocalizations (Figure 1e) and the fear calls (Figure 1f) show that cortically evoked ultrasonic vocalizations had substantial latencies, in the cases shown the median latencies were 67 and 137 ms, respectively. Given the abundance of electrically evoked calls, the total absence of non-natural calls or sounds was a notable observation. Our data show that a variety of natural vocalizations can be evoked from rat medial prefrontal cortex.

## 3.2 | Areal distribution of microstimulation-evoked vocalizations

How do evoked vocalizations map onto areas of rat prefrontal cortex? We observed a similar distribution of responsive (vocalization evoking) and nonresponsive sites in all five mapping experiments. A representative microstimulation map for vocalizations is shown in Figure 2a. Here, we reconstructed seven microstimulation tracks and we show nonresponsive sites marked by x and responsive sites marked by dots. The sites are shown on a color-coded map of cortical areas in parasagittal view. All areal locations of stimulation sites and rostro-caudal coordinates of tracks were histologically verified. In this example rat and in others we observed few vocalization responses to stimulation in dorsal areas (vibrissa motor cortex, secondary motor cortex), far anterior areas (orbital cortex) and ventro-medial areas (infralimbic and dorsopeduncular cortex); however, stimulation-evoked responses were common in prelimbic cortex and cingulate area 2 (Figure 2a). Maps of response (electrically evoked vocalization) probability averaged across experiments lead to similar conclusions (Figure 2b). We analyzed four animals in total and 261 sites (we excluded one animal in this analysis due to failed reconstruction of tracks). The experiments that were designed for our laminar analysis in prelimbic cortex (data shown in Figure 3) were not included in this analysis because only deep layers were targeted for areal comparison. To compute response probability, we aligned sites histologically to the coordinates provided in the Paxinos and Watson atlas, binned them in 0.5 mm (rostro-caudal direction) × 1 mm (depth) bins and computed the fraction vocalization evoking stimulation sites in the respective bin. Vocalizations were common over posterior prelimbic and cingulate area 2, but less frequent dorsally, anterior and ventral from these areas (Figure 2b). A precise breakdown of responsive and unresponsive sites per area is given in Figure 2c. There were significant differences in responsiveness between areas (Chi-squared test, $p < 0.00001$), with significantly more responsive sites in prelimbic cortex than in many other areas (cingulate area 1 (47 sites tested), vibrissa motor cortex (22 sites tested), secondary motor cortex (29 sites tested): Fisher's exact test, $p < 0.001$; medial- and ventral-orbital area (26 sites tested): Fisher's exact test, $p < 0.05$). It was also the case that within the prelimbic area responsiveness seemed to differ. We observed a significantly larger fraction of vocalization evoking sites in posterior than in anterior prelimbic cortex ($p = 0.012$ Fisher's exact test, four animals, 79 sites); such differences might justify partitioning prelimbic cortex into an anterior and a posterior division as shown in Figure 2d. In summary, these data suggest that rat medial prefrontal cortical areas differ sharply in the extent to which their stimulation evokes vocalization.

## 3.3 | The amount of responsive sites and the types of evoked vocalizations are different across layers in prelimbic cortex

We wondered whether the probability to evoke vocalizations is different across layers and whether evoked vocalizations in superficial layers are different from deep layers with respect to USV type (fear calls vs. 50 kHz). To test this, we inserted electrodes in prelimbic cortex at four different medio-lateral extents (three rats). Figure 3a shows an example histological section in which all four tracks and some stimulation sites are clearly visible. In the schematic Figure 3b, the four tracks, all responsive (circles) and nonresponsive sites (marked with an x) are depicted in relation to the different layers. A minority of the responsive sites (two out of six, one of them at the border to layer 5) in this experiment were located in superficial layers (layer 2/3), whereas all other responsive sites were found in deeper layers (layers 5 and 6). Both vocalizations that were evoked in superficial layers were classified as fear calls (red circles), whereas three out of the four evoked vocalizations in deep layers were classified as 50 kHz USVs (black circles). To analyze whether such layer dependencies can be found at the population level, we pooled the data from the three rats with post-hoc analyzed prelimbic sections of the data shown in Figure 2c (total after pooling: seven rats). We found significantly more sites at which vocalizations could be evoked in deeper layers compared to superficial layers (Figure 3c, 50/94 tested sites (deep) versus 6/55 tested sites (superficial); $p < 0.0001$, Fishers exact test). The few sites in superficial layers were almost exclusively classified as fear calls (Figure 3d left, 5/6 of responsive sites) and this was significantly different from sites in deep layers, where mostly 50 kHz calls were evoked (Figure 3d right, 40/50 of responsive sites; $p < 0.05$, Fishers exact test). These results suggest that deep layers of the prelimbic cortex have greater access to the initiation of vocalizations (mainly 50 kHz) than superficial layers but that superficial layers might be involved in the generation of fear calls.

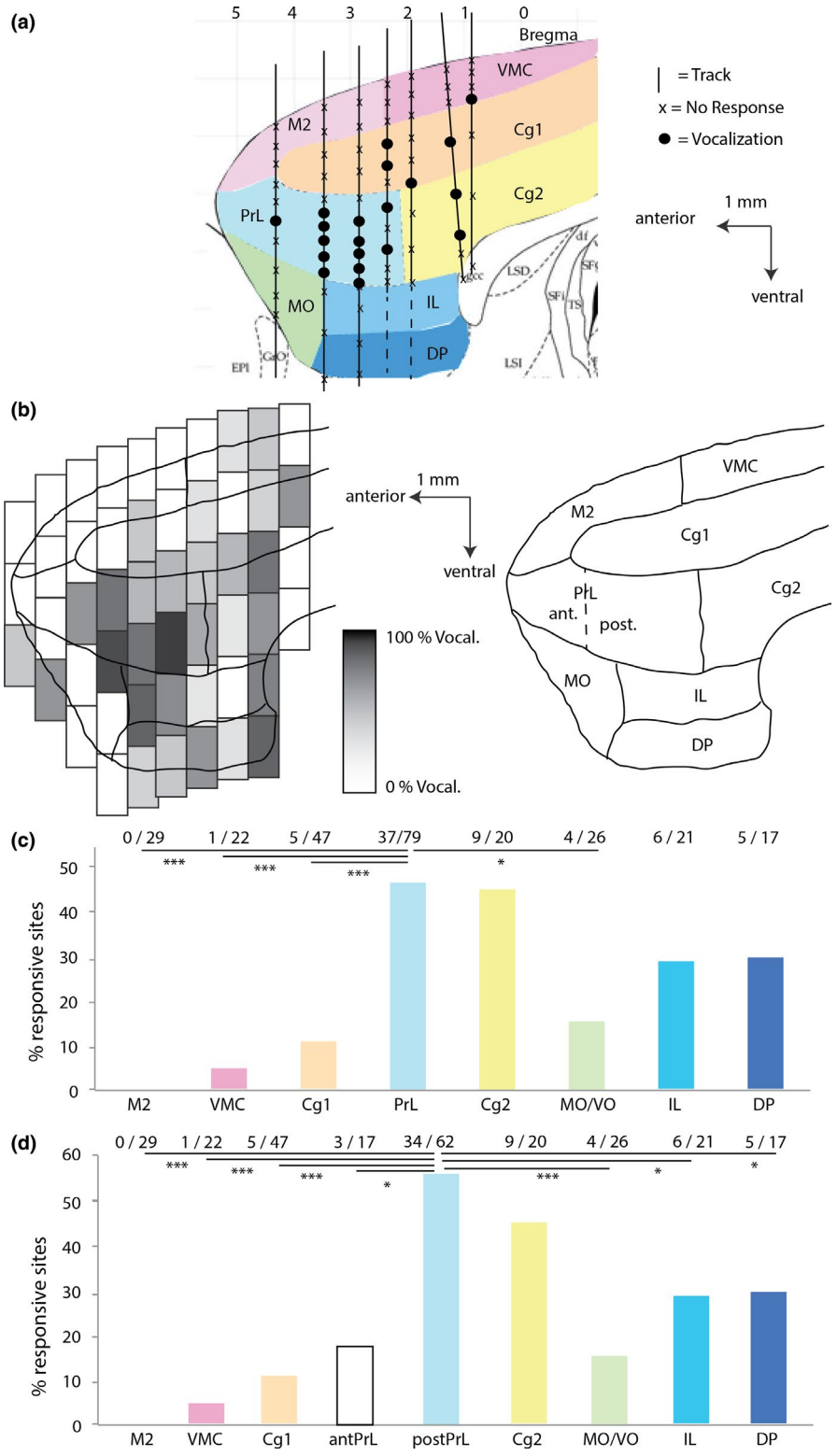


## 3.4 | A variety of vocalizations are evoked, which match with naturally occurring calls

What kind of vocalizations was evoked by microstimulation in rat frontal cortices? We found that a wide variety of vocalizations could be evoked in rat frontal cortices (Figure 4). The calls evoked included modulated calls (Figure 4a left and middle), bow calls (Figure 4b left and middle), combined calls (Figure 4c left and middle), ramp up calls (Figure 4d left and middle) and fear calls (Figure 4e left and middle). We have extended experience with naturally occurring rat vocalizations (Ishiyama & Brecht, 2016; Rao et al., 2014) and found that electrically evoked calls without exception matched with naturally occurring rat vocalizations. As shown

**FIGURE 2** Areal distribution of microstimulation-evoked vocalizations evoked in rat frontal cortex. (a) microstimulation map of evoked vocalizations in the frontal cortex of a rat. Nonresponsive sites (x) and vocalization evoking sites (black dots) were studied in seven tracks and after histological verification were superimposed on a parasagittal section with color-coded cortical areas. For all tracks, the stimulation electrode was inserted 0.75 mm lateral from bregma. Most but not all vocalization evoking sites fall into the prelimbic (PrL) and cingulate area 2 (Cg2) areas. Other abbreviations: cingulate area 1 (Cg1); secondary motor cortex M2; vibrissa motor cortex (VMC); medial-orbital area (MO); ventral-orbital area (VO), infralimbic cortex (IL); dorsopenducular cortex (DP). The areal boundaries were drawn according to Paxinos & Watson, 1986 and Brecht et al., 2004. (b) left, average map vocalization responsiveness superimposed on a parasagittal section ($n = 4$ animals). Right, outline of cortical area boundaries for reference. The dashed line indicates an alternative portioning scheme, that is, a split of the prelimbic area split into an anterior portion (antPrL) and a posterior portion (postPrL). When superimposing stimulation tracks on an average maps, we adjusted for histologically correct rostro-caudal coordinates. We also factored in that in the 1 mm stimulation electrodes did only travel about 0.5 mm due to dimpling; hence we aligned tracks at +0.5 mm relative to the cortical surface. Conventions as in (a). (c) areal distribution of nonresponsive and vocalization evoking sites (expressed as fraction of vocalization evoking sites) across areas of frontal cortex. The numbers on top of the columns refer to the number of vocalization evoking sites and total number of histologically assigned sites, respectively. Data refer to four animals in which in total 261 sites were tested. The value from the Chi-squared test was >43.3, $p < 0.00001$. We also compared the distribution of nonresponsive and vocalization evoking sites between prelimbic cortex (the area with the largest fraction of vocalization sites) and the other cortical areas with Fisher's exact test and found significant differences to four of the seven areas (**$p < 0.001$; *$p < 0.05$). Abbreviations as in (a), MO/VO pooled data from medial-orbital and ventral-orbital cortex. (d) areal distribution of nonresponsive and vocalization evoking sites with a split prelimbic area as indicated by the dashed line in right hand schematic in (b). The numbers on top of the columns refer to the number of vocalization-evoking sites and total number of histologically assigned sites, respectively. Data refer to four animals in which in total 261 sites were tested. The value from the Chi-squared test was >51.3, $p < 0.00001$. We also compared pairwise the distribution of nonresponsive and vocalization evoking sites between prelimbic cortex (the area with the largest fraction of vocalization sites) and the other cortical areas with Fishers exact test and found significant differences to four of the seven areas (**$p < 0.001$; *$p < 0.05$). [Colour figure can be viewed at wileyonlinelibrary.com]

in Figure 4 for each electrically evoked call (Figure 4a–e left and middle) a corresponding very similar call (Figure 4a–e right) could be found in our samples of natural calls. There were no systematic differences in the frequency of natural and electrically evoked calls.

## 3.5 | Vocalization thresholds, latencies and call types

Next, we considered the characteristics of microstimulation-evoked vocalizations (Figure 5). As shown in Figure 5a, thresholds for evoking vocalizations were high. We tested current intensities between 10 and 500 μA and across areas the mean threshold was 390 ± (160 *SD*) μA. For the areas, for which we obtained at least five threshold values, we compared thresholds by an ANOVA analysis. There were no significant differences in stimulation threshold across areas (*f*-ratio = 0.10777; $p = 0.955164$, four animals, 62 sites). A histogram of latencies of all evoked calls is shown in Figure 5b. Latencies were substantial, virtually none were below 25 ms and the median latency was 175 (± 185 *SD*) ms. We broadly categorized stimulation sites according to the calls they evoked as 50 kHz call sites (see Figure 1c) or as fear call evoking sites (see Figure 1d) or as mixed sites, where both call types were evoked (Figure 5c). Fifty kHz sites dominated. We note that more refined call categorization schemes have been proposed (Litvin, Blanchard, & Blanchard, 2007) and head-fixation—a procedure stressful to the animals—may have biased vocalizations toward fear calls. In most cases, calls were locked to the onset of stimulation rather than to stimulation offset (Figure 5d). Stimulation studies in the motor system have typically found that in structures close to the motor output, stimulation thresholds are low and movement latencies are short. Hence, the high thresholds and long latencies to vocalization observed in medial prefrontal cortex might suggest this structure is only indirectly linked to vocalizations.

## 3.6 | Anterograde tracing

In order to understand the anatomical underpinnings of how posterior prelimbic cortex contributes to vocalizations, we performed anterograde tracing experiments. To this end, we injected the tracer Biotinylated Dextran Amine (BDA; Molecular Weight: 10,000, a potent anterograde tracer) into posterior prelimbic cortex (Figure 6a) of two rats; the BDA injection was limited to posterior prelimbic cortex in both cases investigated. In both analyzed brains, we found that posterior prelimbic cortex projects to a limited set of cortical targets. Most notable were projections to cingulate area 2 (Figure 6b), an area in which electric stimulation also evoked numerous vocalizations. Other cortical areas that received weaker projections were the ventral orbitofrontal cortex, infralimbic cortex, cingulate area 1 and retrosplenial cortex (Figure 6c), also see Table 1. Posterior prelimbic cortex targeted a huge number of subcortical targets, which included the nucleus accumbens (Figure 6a), the striatum (Figure 6b), the habenula and medial dorsal thalamus (Figure 6c), the periaqueductal

gray (Figure 6d) and many other targets including neuromodulatory centers such as the raphe nuclei and the ventral tegmental area (Table 1).

## 3.7 | Anterograde transsynaptic tracing

The periaqueductal gray is a target structure of prelimbic cortex with potential functional significance for vocalization generation. The projections of posterior prelimbic cortex to the periaqueductal gray are noteworthy in the context of our study, since the periaqueductal gray is a key structure in vocalization control in mammals (Jürgens, 1994). As the periaqueductal gray is also involved in many other functions, the functional significance of projections of posterior prelimbic cortex to the periaqueductal gray needs to be further investigated. To this end, we chose a disynaptic tracing approach, which allowed us to assess if the periaqueductal gray neurons targeted by posterior prelimbic cortex did indeed project to putative vocal pattern generator regions in the brain stem such as the intermediate reticular formation (Hage & Jürgens, 2006; Jürgens & Hage, 2007) and the nucleus retroambiguus (Holstege, 1989). To clarify these matters, we adopted the transsynaptic labeling procedure from Zingg et al. (2016). In this transsynaptic labeling approach, presynaptic neurons (in our case in the prelimbic area) are virally induced to express Cre-recombinase and a nuclear fluorescent reporter (in our case red fluorescent protein, RFP). The virus is taken up by postsynaptic neurons (in our case neurons in the periaqueductal gray) again leading to the expression of Cre-recombinase and RFP. Due to the low efficacy of the transsynaptic spread, we expected red nuclear fluorescence to be weak or below detection threshold in postsynaptic neurons. However, due to the high enzymatic efficacy of Cre-recombinase, postsynaptic neurons can be visualized by infecting these cells with another virus that enables Cre-dependent expression of a cytosolic fluorescent reporter (in our case GFP). The cytosolic expression of this Cre-dependent fluorescent reporter allows the visualization of soma, dendrites and axonal projections of these neurons. To do this, we injected an AAV1.Syn.iCre.RFP virus (Figure 7a, left), which induced nuclear red fluorescence and the production of Cre-recombinase in prelimbic cortex in both injected rats (example section shown in Figure 7a, middle and right). Note that presynaptic neurons just show nuclear fluorescence and hence the processes and axonal projections are not visible (Figure 7a, right; nuclear RFP). According to Zhao et al. (2017), a smaller fraction of overload viral particles are presumably anterogradely and transsynaptically transported and induced expression of Cre-recombinase in postsynaptic neurons. We then injected an AAV1.CAG.flex.GFP virus into the periaqueductal gray (Figure 7b, left) leading to Cre-dependent green fluorescent protein expression in two out of two analyzed brains (Figure 7b, middle and right). As expected, we could not detect nuclear RFP in periaqueductal gray cells

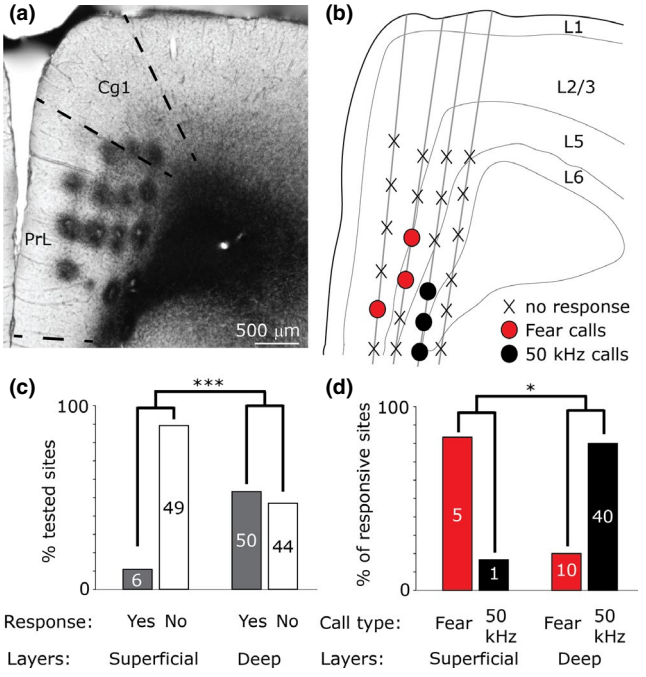


**FIGURE 3** Both microstimulation efficacy and evoked call types differ between superficial and deep layers of prelimbic cortex. (a) Histological example of multiple tracks and microstimulation sites in the prelimbic cortex of a coronal section. (b) Schematic of the micrograph shown in (a) depicting all four tracks (gray) and all 24 microstimulation sites in relation to the different layers (calls on the border between L2/3 and 5 were always assigned to superficial layers). The circles indicate responsive sites and nonresponsive sites are marked with an x. Note that in this example most responsive sites (4/6) were found in deep layers and most of them evoked 50 kHz calls (3/4, black circles) but that sites in superficial layers exclusively (2/2, red circles) evoked fear calls. (c) Responsiveness population data of experiments designed for laminar analysis in the prelimbic cortex (three rats, 72 sites) pooled with prelimbic cortex data that are shown in Figure 2c (four rats, 77 sites; layers were post-hoc assigned, two sites were excluded because layer assignment was not possible). Left, bar graphs show the fraction of responsive (gray bars) and nonresponsive (white bars) sites relative to the total number of sites tested within that layer. The numbers in the bar graphs indicate the absolute numbers of responsive and nonresponsive sites. Right, same as left but for deep layers. Note that it was much more likely to evoke calls in deep layers than in superficial layers (***$p < 0.0001$, Fishers exact test). (d) Call type population data of evoked call types of experiments designed for laminar analysis in prelimbic cortex (three rats, 17 responsive sites, mixed calls were excluded) pooled with prelimbic cortex data that are shown in Figure 2c (4 rats, 39 responsive sites, layers were post-hoc assigned). Left, bar graphs show the fraction of sites that evoked fear and 50 kHz calls relative to the total number of responsive sites within that layer. The numbers in the bar graphs indicate the absolute numbers of sites that evoked fear or 50 kHz calls, respectively. Right, same as left but for deep layers. Note that microstimulation in deep layers by and large evoked 50 kHz calls. In contrast, almost exclusively fear calls were evoked at the few responsive sites in superficial layers, indicating that the types of evoked calls are different between superficial and deep layers (*$p < 0.05$, Fishers exact test). [Colour figure can be viewed at wileyonlinelibrary.com]

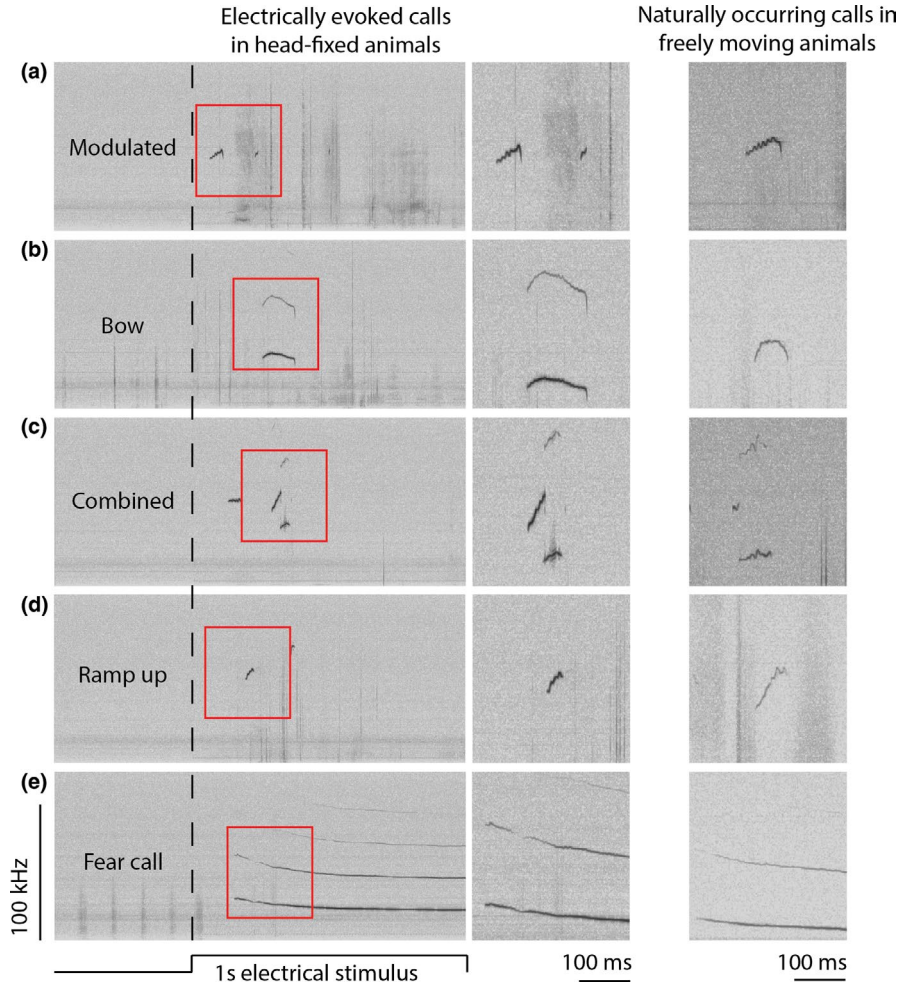


**FIGURE 4** Comparison of electrically evoked (left) and naturally occurring (right) USVs. (a) Left, microstimulation-evoked modulated calls are within the 50–60 kHz range and show strong rippled frequency modulation during the rising phase of the call. Middle, high-time resolution spectrogram of the same call. Right, a similar call observed during natural play behavior. (b) Left, microstimulation-evoked bow call: This call has a rising and a falling phase but it is not frequency-modulated as shown in **A**. Middle, high-time resolution spectrogram of the same call. Right, a similar bow call observed during natural play behavior. (c) Left, microstimulation-evoked combined call typically showing two components: A first 50–60 kHz call, immediately followed by a 45 kHz call with its 90 kHz harmonic. Middle, high-time resolution spectrogram of the same call. Right, a similar combined call observed during natural play behavior. (d) Left, microstimulation-evoked ramp up call, characterized by a rising phase but without falling phase. Middle, high-time resolution spectrogram of the same call. Right, a similar call observed during natural play behavior. (e) Left, microstimulation-evoked fear call. These calls are long, continuous USVs in the 22 kHz range with multiple harmonics. They start at about 30 kHz and approach 22 kHz with time as shown in electrically induced and natural fearful conditions. Middle, high-time resolution spectrogram of the initial parts of the same call. Right, a similar call emitted by a fearful animal. [Colour figure can be viewed at wileyonlinelibrary.com]

of both rats (Figure 7b, right) like we did in the prelimbic starter neurons, probably due to sparse transsynaptic spread of the virus and hence low expression levels in postsynaptic neurons. Consistent with a role of these neurons in vocalization control, we found for both analyzed animals that these cells projected heavily to intermediate reticular formation (Figure 7c), a key structure in vocalization control (Hage & Jürgens, 2006; Jürgens & Hage, 2007) and weakly also to the nucleus retroambiguus and the surrounding reticular formation (Figure 7d). To ensure that AAV1.CAG.flex.GFP was only capable to express GFP in Cre-expressing cells, we performed a control injection of this virus in one rat without prior AAV1.Syn.iCre.RFP injection in the prelimbic cortex (Figure 7e). As expected, GFP-expressing cells were absent in all analyzed sections. In summary, these data demonstrate a disynaptic link from prelimbic cortex through the periaqueductal gray to vocal pattern generating structures (Figure 7f).

## 4 | DISCUSSION

### 4.1 | Summary

We applied microstimulation mapping for evoked vocalizations procedures and identified numerous vocalization evoking sites in rat medial-prefrontal-anterior cingulate cortex. Frontal cortical areas differ markedly in the fraction of vocalization

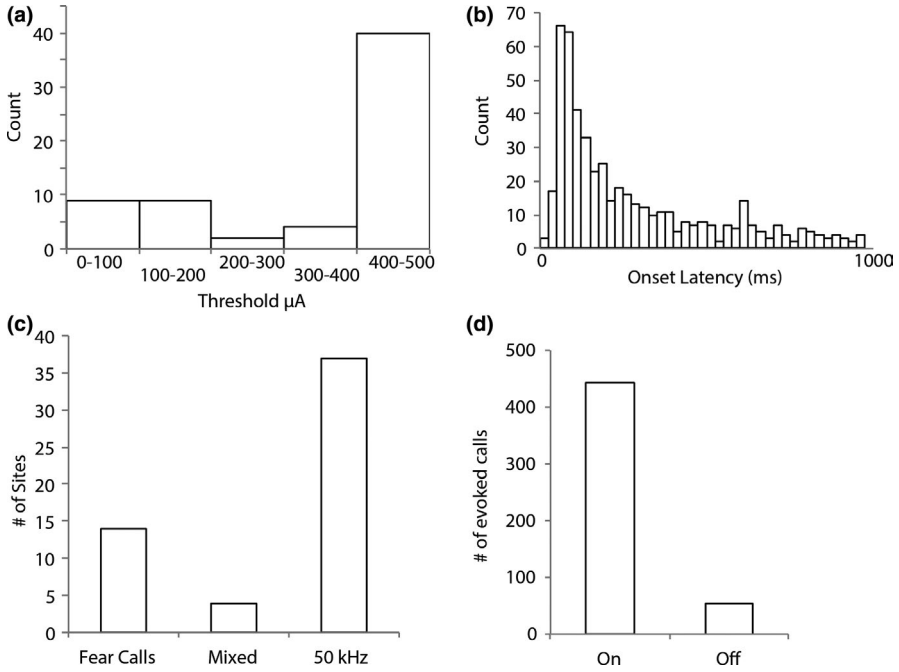


**FIGURE 5** Vocalization thresholds, vocalization latencies, call types and response types. (a) distribution of stimulation thresholds for evoking vocalizations. Note that these data refer only to the subset of stimulation sites, at which calls were evoked. There were no significant differences in thresholds between different areas and we therefore pooled all data (ANOVA, *f*-ratio = 0.10777; $p = 0.955164$, 62 sites, four animals). There were only few <100 µA threshold sites. (b) latencies of all stimulation-evoked vocalizations. Data are shown in 25 ms bins. Note the almost complete absence of < 25 ms latencies, and the small number of < 50 ms latencies. (c) evoked call types. Note that these data refer only to the subset of stimulation sites, at which calls were evoked. As fear call sites, we classified sites, where microstimulation evoked characteristic long and loud calls in the 20–30 kHz range; as 50 kHz calls sites we classified sites, where a diversity of calls in the 30–100 kHz range was evoked; as mixed sites we classified sites, where microstimulation evoked both types of calls. (d) on and off response patterns. Note that these data refer only to the subset of stimulation sites, at which calls were evoked. As on-calls, we classified calls evoked during the 1 s stimulation train. As off-calls we classified calls evoked in the first second after the end of the stimulation train

evoking sites and the posterior prelimbic area and cingulate area 2 form hotspots for vocalizations. In these two areas, a great variety of naturally occurring calls were evoked, albeit at high thresholds and with long latencies. Posterior prelimbic cortex has a wide variety of projection targets and connects disynaptically to brainstem vocalization centers.

## 4.2 | Vocalizations evoked in rat medial-prefrontal-anterior cingulate cortex

Microstimulation in the medial-prefrontal-anterior cingulate cortex of awake head-fixed animals evoked vocalizations in all five rats. The results were consistent across animals with respect to areal distribution and thresholds. Our data confirm and greatly extend earlier evidence that pointed to a role of rodent prefrontal cortex in vocalization control. Such earlier data include, scattered vocalizations evoked by electric stimulation in rat frontal cortex (Burgdorf et al., 2007), responses to vocalizations in rat anterior cingulate cortex (Saito & Okanoya, 2017), vocalizations evoked by electric stimulation in the frontal cortex of anesthetized guinea pigs (Green et al., 2018) and the abolition of fear calls by lesions to frontal cortex (Frysztak & Neafsey, 1991). It appears that electrically evoked calls were more common in our study than in previous work. The higher incidence of vocalization might be related to the fact that we applied the stimulation in awake rather than anesthetized animals (Green et al., 2018) and that we applied higher current intensities (Burgdorf et al., 2007). A potential limitation of our microstimulation work is the use of head-fixation, a procedure stressful to the experimental animals, which may have also altered the animal's calling behavior.

## 4.3 | Areal distribution of vocalization sites

Cortical areas greatly differed in the fraction of sites, which electrically drove vocalizations. In particular, we found that stimulation drove vocalization at many sites of prelimbic cortex and cingulate area 2. Within the area assigned as prelimbic cortex by the Paxinos and Watson rat atlas (1986), there were large differences between anterior prelimbic cortex (at coordinates ≥4 mm anterior to bregma, where few vocalizations were evoked) and posterior prelimbic cortex (at coordinates <4 mm anterior to bregma, where many vocalizations were evoked). Retrograde tracing by other authors revealed strong

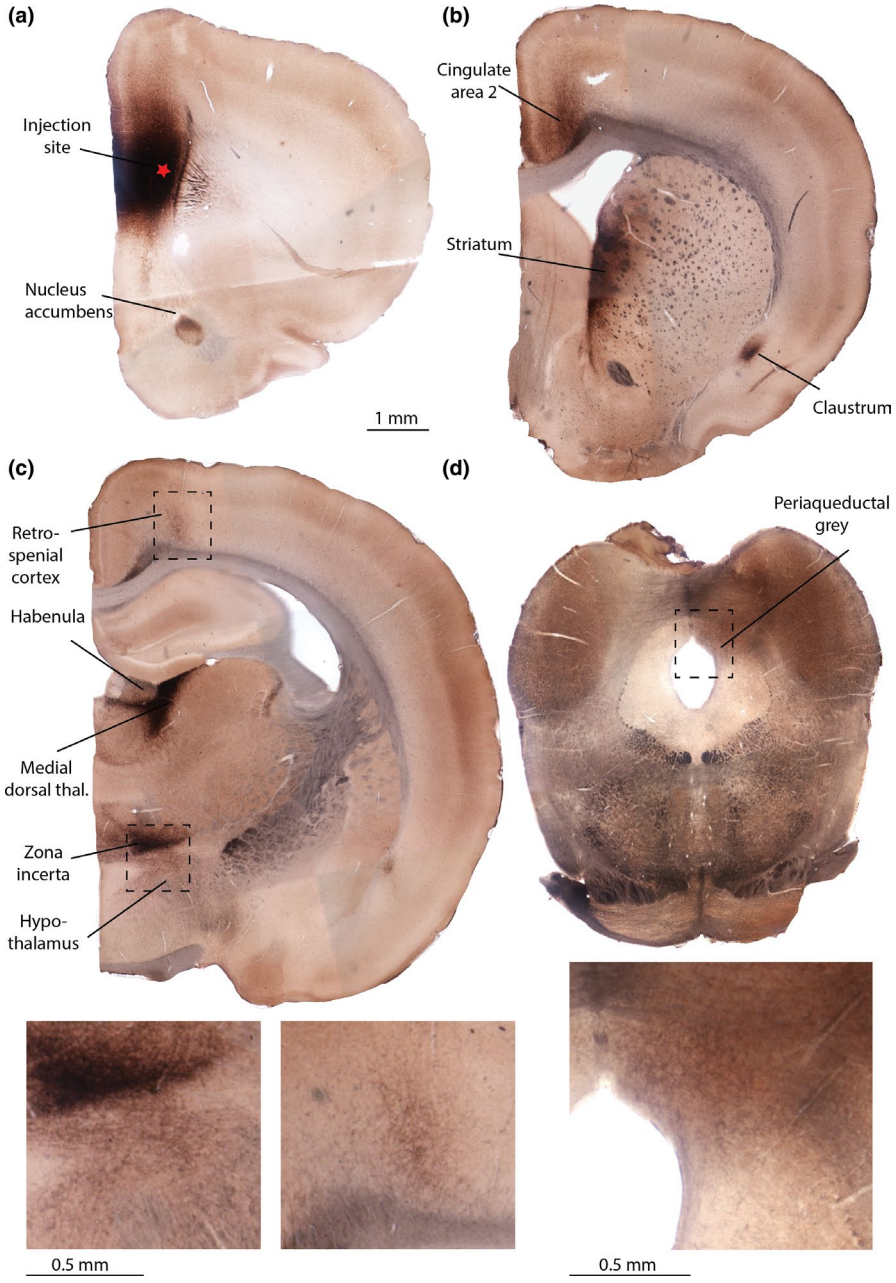


**FIGURE 6** Projections of posterior prelimbic cortex revealed by anterograde tracing. (a) Injection site of the tracer biotinylated dextran amine (BDA; Molecular Weight: 10,000, a potent anterograde tracer) in posterior prelimbic cortex (PrL). The injection site is marked with a red star. The nucleus accumbens is a prominent projection target of prelimbic cortex and is revealed by dark axonal staining. (b) in a more posterior section anterograde labeling in cingulate area 2 (Cg2) and the striatum are visible. (c) Top, further posterior cortical labeling is seen in retrosplenial cortex (surrounded by a dashed box and shown enlarged at the bottom right micrograph. Labeling is also seen in the habenula, medial dorsal thalamus and the zona incerta/the dorsal hypothalamus (surrounded by a dashed box and shown enlarged at the bottom left micrograph). (d) Top, midbrain section with labeling in the periaqueductal gray (dashed box). Bottom, enlarged view of labeled axons in the periaqueductal gray. [Colour figure can be viewed at wileyonlinelibrary.com]

connections from cingulate area 2 (where we also evoked numerous vocalizations) to posterior prelimbic cortex, whereas the connections from anterior to posterior prelimbic cortex were weak (Conde, Maire-Lepoivre, Audinat, & Crepel, 1995). Additional functional and anatomical work should be directed to the question, if anterior and posterior prelimbic cortex form two distinct cortical areas. Our laminar analysis revealed that vocalizations were much more often elicited in deep layers of prelimbic cortex, which was expected as prelimbic layer 5 is known to project to the periaqueductal gray (Cheriyan, Kaushik, Ferreira, & Sheets, 2016). Additionally to the quantitative difference of responsive sites, we also observed qualitative differences regarding call types: The majority of evoked calls in deep layers were in the 50 kHz range, which are associated with positive affect. In contrast, at the few responsive sites in superficial layers we observed almost exclusively 22 kHz evoked calls, which are associated with fear or negative effect. Interestingly, superficial layers are known to project to the amygdala, whereas deep layers project to the ventral tegmental area (Murugan et al., 2017). It is tempting to speculate that the generation of 22 kHz calls is at least partly mediated by amygdala projecting prelimbic neurons, whereas the generation of 50 kHz calls might be facilitated by ventral tegmental area projecting prelimbic neurons.

## 4.4 | Anatomical underpinnings of vocalization control by prelimbic cortex

Our anterograde and anterograde-transsynaptic tracing also provide insights as to how prelimbic cortex might

**TABLE 1** Projection Targets of posterior Prelimbic Cortex assessed with anterograde tracing with Biotinylated Dextran Amine

| | Projection strength |
|---|---|
| Cortical targets | |
| Ventral orbitofrontal cortex | + |
| Cingulate area 1 | + |
| Cingulate area 2 | ++ |
| Infralimbic cortex | + |
| Retrospenial cortex | + |
| Subcortical targets | |
| Anterior olfactory nucleus | + |
| Nucleus accumbens core | ++ |
| Nucleus accumbens shell rostral and caudo-ventral | + |
| Nucleus accumbens shell caudo-medial | ++ |
| Claustrum | ++ |
| Medial striatum | ++ |
| Lateral septum | + |
| Ventral pallidum | + |
| Bed nucleus | + |
| Medial and lateral preoptic area | + |
| Paraventricular/paratenial thalamic nucleus | + |
| Anteromedian thalamic nucleus | ++ |
| Globus Pallidus | ++ |
| Anterior/lateral hypothalamus | + |
| Habenula | ++ |
| Reticular thalamus | ++ |
| Reuniens thalamic nucleus | ++ |
| Anterodorsal thalamic nucleus | ++ |
| Zona incerta | ++ |
| Amygdala | ++ |
| Periaqueductal gray dorsal | ++ |
| Periaqueductal gray ventral | + |
| Substantia nigra/ventral tegmental area | + |
| P1 reticular formation | + |
| Parabrachial pigmented nucleus | + |
| Superior colliculus deep | + |
| Pons | + |
| Paramedian raphe nuclei | ++ |
| Dorsal raphe nuclei | + |
| Laterodorsal tegmental nucleus | + |
| Dorsomedial tegmental area | + |
| Barringtons nucleus | + |
| Central gray of the pons | + |

+ indicates weak projections (rarely intersecting fibers visible).
++ indicates strong projections (heavily intersecting fibers visible forming a clear projection spot).

control vocalizations. Consistent with earlier work (Vertes, 2004), we find that prelimbic cortex has a limited number of cortical targets and numerous subcortical targets. With respect to vocalization control, the most obvious prelimbic target of relevance is the periaqueductal gray. The periaqueductal gray has long been recognized as a key control structure for vocalizations in monkeys (Jürgens, 1994) but also in rats (Yajima, Hayashi, & Yoshii, 1980). While

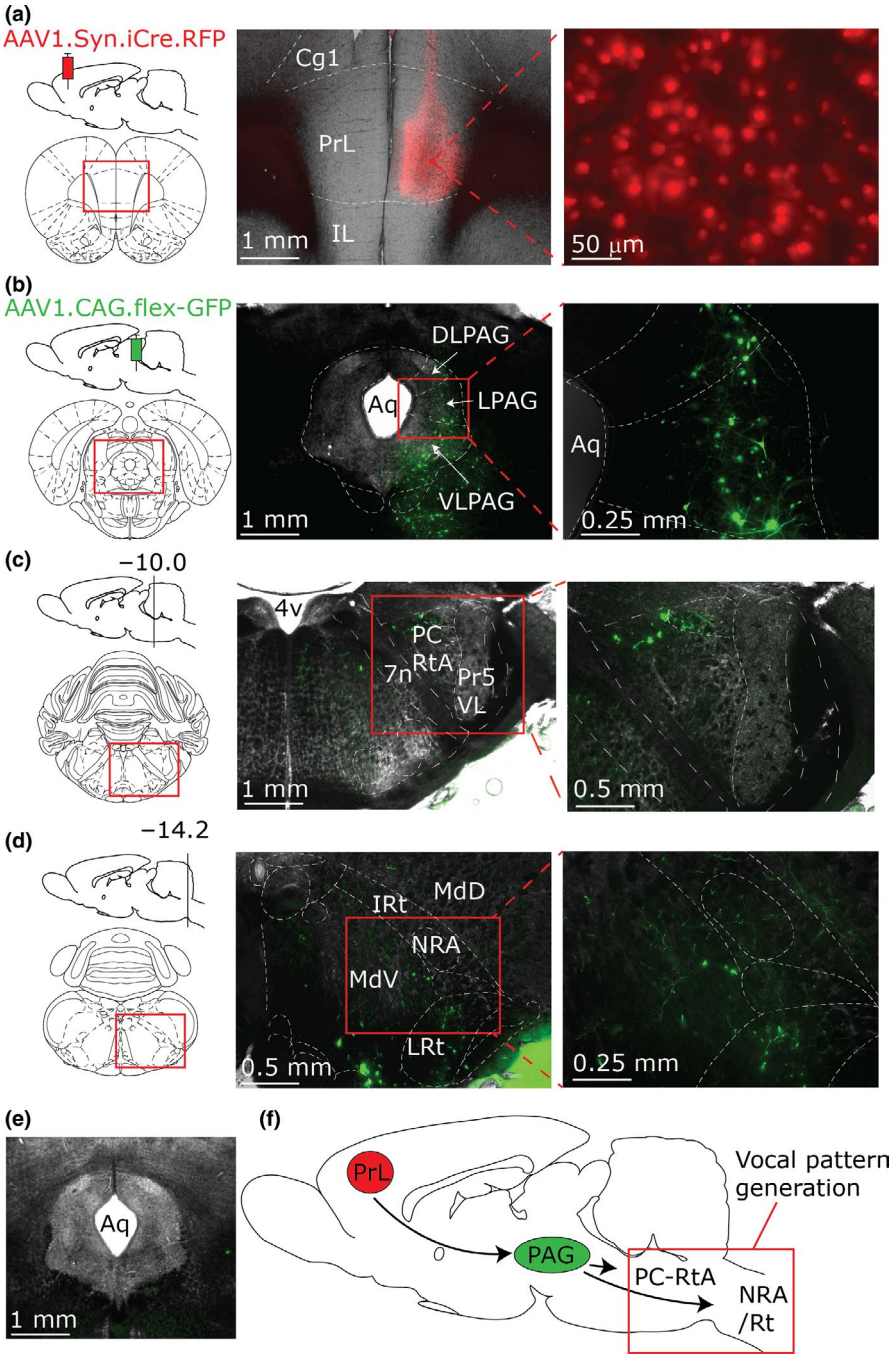


our anterograde tracing results largely confirm the earlier work (Vertes, 2004), our interpretation of the connectivity results differs from that of Vertes. Specifically, Vertes suggested that prelimbic cortex might be homologous in connectivity to primate dorsolateral prefrontal cortex. We instead highlight that the connectivity of rat prelimbic cortex is similar to the connectivity of vocalization areas in monkey anterior cingulate cortex as described by Müller-Preuss and Jürgens (1976). Much like the rat prelimbic cortex, the monkey anterior cingulate cortex has a limited set of cortical targets, which include neighboring cingulate areas and orbitofrontal cortex. Additionally many subcortical targets are shared between monkey anterior cingulate cortex and rat prelimbic cortex. Common targets include the striatal structures, amygdala, habenula, claustrum and periaqueductal gray. The results of our anterograde transsynaptic tracing support the idea of a control of vocalizations by prelimbic cortex via the periaqueductal gray. We find that periaqueductal gray neurons innervated by prelimbic cortex strongly project to brainstem nuclei involved in vocal pattern generation such as the intermediate reticular formation (Hage & Jürgens, 2006; Jürgens & Hage, 2007) and the nucleus retroambiguus (Holstege, 1989). A recent study supports the idea that periaqueductal

**FIGURE 7** Anterograde transsynaptic viral tracing reveals a prelimbic cortex—periaqueductal gray—brainstem vocalization centers circuit. (a) Prelimbic (PrL) injection site of the AAV1.Syn.iCre.RFP used for anterograde transsynaptic tracing. Left, parasagittal and coronal scheme of the AAV1.Syn.iCre.RFP injection at + 3 mm from Bregma. Middle, micrograph of the AAV1.Syn.iCre.RFP injection site in the PrL showing Cre-expressing cells (red). Cg1, cingulate cortex, area 1; PrL, prelimbic cortex; IL, infralimbic cortex. Right, magnification of micrograph shown in the middle panel (the picture was acquired as a stack image that was collapsed such that nuclei appear in one focal plane). Note that RFP expression is restricted to the putative nuclei (small, circumscribed spheres with a week halo) due to a nuclear translocation sequence—thereby no neuronal processes are visible. (b) Anatomical location of the periaqueductal (PAG). Left, parasagittal and coronal scheme of the Cre-dependent AAV1.CAG.flex.GFP injection at −7.8 mm from Bregma. Middle, micrograph of the AAV1.CAG.flex.GFP injection site in the PAG showing Cre-dependent GFP-expressing neurons (green) that receive input from PrL. DLPAG, dorsolateral periaqueductal gray; LPAG, lateral periaqueductal gray; VLPAG, ventrolateral periaqueductal gray; Aq, aqueduct. Right, magnification of micrograph shown in the middle panel. Cytosolic GFP expression allows visualization of axons and dendrites. Note that presynaptic terminals from prelimbic neurons are not visible because the presynaptic reporter (red fluorescent protein) is restricted to the nucleus. (c) Anatomical location at the rostral brainstem level. Left, parasagittal and coronal scheme of the section shown in the middle and right panel at −10 mm from Bregma. Middle, micrograph showing green fluorescent fibers in the PC-RtA (parvocellular reticular formation, alpha part). Pr5VL, principal sensory trigeminal nucleus, ventrolateral part; 7n, facial nerve; 4v, fourth ventricle. Right, magnification of micrograph shown in the middle panel. Note that Green fibers are localized at the dorsal part of the PC-RtA. (d) Anatomical location at the caudal brainstem level. Left, parasagittal and coronal scheme of the section shown in the middle and right panel at −14.2 mm from Bregma. Middle, micrograph showing green fluorescent fibers in the NRA and the surrounding reticular formation. NRA, nucleus retroambiguus; IRT, intermediate reticular nucleus; MdD, medullary reticular nucleus, dorsal part; MdV, medullary reticular nucleus, ventral part; LRt, lateral reticular nucleus. Right, magnification of micrograph shown in the middle panel. Note the diffuse spread of green fluorescent fibers within the NRA and the surrounding reticular formation. (e) Control AAV1.CAG.flex.GFP injection in the periaqueductal gray without AAV1.Syn.iCre.RFP injection in the prelimbic cortex. Note the absence of green fluorescent cells, indicating that the Cre-dependent (flex) virus only leads to GFP expression when Cre-recombinase is expressed. (f) Possible prefrontal cortex to brainstem circuit for vocalization production. The periaqueductal gray (PAG) receives input from the PrL and conveys that information to the brainstem vocal pattern generator nuclei (PC-RtA and NRA/Rt). PC-RtA, parvocellular reticular formation, alpha part; NRA, nucleus retroambiguus; Rt, reticular formation. [Colour figure can be viewed at wileyonlinelibrary.com]

gray neurons projecting to the brainstem gate vocalizations (Tschida et al., 2018). The viral transsynaptic labeling approach developed by Zingg et al. (2016) worked well in our preparation. We observed red nuclear fluorescence of presynaptic prelimbic neurons and GFP labeling in postsynaptic periaqueductal gray neurons, which we had observed to be targeted by our non-viral anterograde tracing. The Cre-dependent transsynaptic tracing works favorably for the analysis of the prelimbic–periaqueductal gray projection, because this unidirectional connection avoids potential confounds that can occur in bidirectional projections (Zingg et al., 2016).

### 4.5 | Prelimbic cortex and cingulate area 2 might contribute to the high-level control of vocalizations

Our observations point to an involvement of prelimbic cortex and cingulate area 2 in vocalization control. This conclusion is suggested by the fact that a wide variety of calls were evoked at a large fraction of stimulation sites in these areas. In all cases, in all animals, we evoked complex calls as naturally emitted by rats. We never observed non-natural calls or sounds, that is, in >1,000 stimulation trials at more than 200 stimulation sites we did not evoke a single non-natural call. Thus, these areas do not seem to directly impact on sound production, but rather seem to determine the emission of complete natural calls. The long latencies and high thresholds suggest the same conclusion, that is, prelimbic cortex and cingulate area 2 are rather distant from sound production. The interpretation that cortical circuits have only a high-level nonessential control function in call production goes with results that show that mice without cortex can produce songs (Hammerschmidt, Whelan, Eichele, & Fischer, 2015). It might be worthwhile to contrast the role of rat motor cortex in movement control with role of prelimbic cortex in vocalization control. In motor cortex stimulation, thresholds for movement (<50 μA, Brecht et al.(2004)) are several times lower than the thresholds for vocalization in prelimbic cortex, latencies for movement are several times shorter (20–40 ms, Matyas et al. (2010)) than latencies for vocalization in prelimbic cortex. Finally motor cortex sends a very heavy projection to somatosensory cortex (Mao et al., 2011), whereas prelimbic cortex does not project to auditory cortex. All of these differences suggest that motor cortex is more directly involved in movement generation than prelimbic cortex is involved in vocalization control.

## 5 | CONCLUSION

The data presented here point to an involvement of rat frontal cortices—in particular posterior prelimbic cortex and cingulate area 2—in vocalization control. These cortices share similarities in anatomical position, connectivity and function to anterior cingulate vocalization areas of cats (Hunsperger & Bucher, 1967) and area 32/area 24 of monkeys (Hughes & Mazurowski,

1962; Jürgens & Ploog, 1970; Smith, 1945). Similar to the pattern sketched for other mammals prelimbic cortex might control vocalization through a periaqueductal gray/brainstem axis. Thus, our data support the idea of fundamental similarities in cortical vocalization control across mammals.

## ACKNOWLEDGEMENTS

We thank Undine Schneeweiß and Tanja Wölk for their outstanding technical assistance; and Konstantin Hartmann for setting up microstimulation procedures and for comments on the manuscript. We also thank Thorsten Trimbuch and Anke Schönherr at the Viral Core Facility, Charité for outstanding support and for provision of the viruses we used for transsynaptic tracing. This work was supported by Humboldt-Universität zu Berlin, BCCN Berlin, NeuroCure and the Gottfried Wilhelm Leibniz-Prize and the German Center for Neurodegenerative Diseases, DZNE.

## CONFLICT OF INTEREST

The authors declare no competing financial interests.

## DATA ACCESSIBILITY

Primary data material can be accessed by contacting the corresponding author.

## AUTHOR CONTRIBUTIONS

P.B and E.M. performed the experiments. P.B., E.M. and M.B. analyzed the data. P.B., E.M. and M.B. wrote the paper.

## ORCID

*Eduard Maier* https://orcid.org/0000-0003-0734-2698

## REFERENCES

Aitken, P. G. (1981). Cortical control of conditioned and spontaneous vocal behavior in rhesus monkeys. *Brain and Language*, *13*(1), 171–184.

Arriaga, G., Zhou, E. P., & Jarvis, E. D. (2012). Of mice, birds, and men: The mouse ultrasonic song system has some features similar to humans and song-learning birds. *PLoS ONE*, *7*(10), e46610.

Brecht, M., Krauss, A., Muhammad, S., Sinai-Esfahani, L., Bellanca, S., & Margrie, T. W. (2004). Organization of rat vibrissa motor cortex and adjacent areas according to cytoarchitectonics, microstimulation, and intracellular stimulation of identified cells. *The Journal of Comparative Neurology*, *479*(4), 360–373.

Brecht, M., & Sakmann, B. (2002). Dynamic representation of whisker deflection by synaptic potentials in spiny stellate and pyramidal cells in the barrels and septa of layer 4 rat somatosensory cortex. *Journal of Physiology*, *543*(Pt 1), 49–70.

Burgdorf, J., Wood, P. L., Kroes, R. A., Moskal, J. R., & Panksepp, J. (2007). Neurobiology of 50-kHz ultrasonic vocalizations in rats: Electrode mapping, lesion, and pharmacology studies. *Behavioral Brain Research*, *182*(2), 274–283.

Cheriyan, J., Kaushik, M. K., Ferreira, A. N., & Sheets, P. L.( 2016). Specific targeting of the basolateral amygdala to projectionally defined pyramidal neurons in prelimbic and infralimbic cortex. *eNeuro*, *3*( 2), ENEURO.0002-16.2016.

Conde, F., Maire-Lepoivre, E., Audinat, E., & Crepel, F. (1995). Afferent connections of the medial frontal cortex of the rat II Cortical and subcortical afferents. *The Journal of Comparative Neurology*, *352*(4), 567–593.

Frysztak, R. J., & Neafsey, E. J. (1991). The effect of medial frontal cortex lesions on respiration, "freezing", and ultrasonic vocalizations during conditioned emotional responses in rats. *Cerebral Cortex*, *1*(5), 418–425.

Green, D. B., Shackleton, T. M., Grimsley, J. M. S., Zobay, O., Palmer, A. R., & Wallace, M. N. (2018). Communication calls produced by electrical stimulation of four structures in the guinea pig brain. *PLoS ONE*, *13*(3), e0194091.

Hage, S. R., & Jürgens, U. (2006). Localization of a vocal pattern generator in the pontine brainstem of the squirrel monkey. *European Journal of Neuroscience*, *23*(3), 840–844.

Hammerschmidt, K., Whelan, G., Eichele, G., & Fischer, J. (2015). Mice lacking the cerebral cortex develop normal song: Insights into the foundations of vocal learning. *Scientific Reports*, *5*, 8808.

Holstege, G. (1989). Anatomical study of the final common pathway for vocalization in the cat. *The Journal of Comparative Neurology*, *284*(2), 242–252.

Hughes, J. R., & Mazurowski, J. A. (1962). Studies on the supracallosal mesial cortex of unanesthetized, conscious mammals. II. Monkey. A. Movements elicited by electrical stimulation. *Electroencephalography and Clinical Neurophysiology*, *14*, 477–485.

Hunsperger, R. W., & Bucher, V. M. (1967). Affective behaviour by electrical stimulation in the forebain and brain stem of the cat. *Progress in Brain Research*, *27*, 103–127.

Ishiyama, S., & Brecht, M. (2016). Neural correlates of ticklishness in the rat somatosensory cortex. *Science*, *354*(6313), 757–760.

Jürgens, U. (1994). The role of the periaqueductal grey in vocal behaviour. *Behavioral Brain Research*, *62*(2), 107–117.

Jürgens, U. (2002). Neural pathways underlying vocal control. *Neuroscience and Biobehavioral Reviews*, *26*(2), 235–258.

Jürgens, U., & Hage, S. R. (2007). On the role of the reticular formation in vocal pattern generation. *Behavioral Brain Research*, *182*(2), 308–314.

Jürgens, U., & Ploog, D. (1970). Cerebral representation of vocalization in the squirrel monkey. *Experimental Brain Research*, *10*(5), 532–554.

Jürgens, U., & von Cramon, D. (1982). On the role of the anterior cingulate cortex in phonation: A case report. *Brain and Language*, *15*(2), 234–248.

Kirzinger, A., & Jürgens, U. (1982). Cortical lesion effects and vocalization in the squirrel monkey. *Brain Research*, *233*(2), 299–315.

Knutson, B., Burgdorf, J., & Panksepp, J. (2002). Ultrasonic vocalizations as indices of affective states in rats. *Psychological Bulletin*, *128*(6), 961–977.

Litvin, Y., Blanchard, D. C., & Blanchard, R. J. (2007). Rat 22 kHz ultrasonic vocalizations as alarm cries. *Behavioral Brain Research*, *182*(2), 166–172.

Mao, T., Kusefoglu, D., Hooks, B. M., Huber, D., Petreanu, L., & Svoboda, K. (2011). Long-range neuronal circuits underlying the interaction between sensory and motor cortex. *Neuron*, *72*(1), 111–123.

Matyas, F., Sreenivasan, V., Marbach, F., Wacongne, C., Barsy, B., Mateo, C., … Petersen, C. C. (2010). Motor control by sensory cortex. *Science*, *330*(6008), 1240–1243.

Müller-Preuss, P., & Jürgens, U. (1976). Projections from the 'cingular' vocalization area in the squirrel monkey. *Brain Research*, *103*(1), 29–43.

Murugan, M., Jang, H. J., Park, M., Miller, E. M., Cox, J., Taliaferro, J. P., … Witten, I. B. (2017). Combined social and spatial coding in a descending projection from the prefrontal cortex. *Cell*, *171*(7), 1663–1677, e1616.

Öngür, D., & Price, J. L. (2000). The organization of networks within the orbital and medial prefrontal cortex of rats, monkeys and humans. *Cerebral Cortex*, *10*(3), 206–219.

Panksepp, J., & Burgdorf, J. (2003). "Laughing" rats and the evolutionary antecedents of human joy? *Physiology & Behavior*, *79*(3), 533–547.

Paus, T. (2001). Primate anterior cingulate cortex: Where motor control, drive and cognition interface. *Nature Reviews Neuroscience*, *2*(6), 417–424.

Paxinos, G., & Watson, C. (1986). *Atlas of the rat brain in stereotaxic coordinates*. New York, NY: Academic Press.

Rao, R. P., Mielke, F., Bobrov, E., & Brecht, M.( 2014). Vocalization-whisking coordination and multisensory integration of social signals in rat auditory cortex. *eLife*, *3*, e03185.

Saito, Y., & Okanoya, K. (2017). Response characteristics of the rat anterior cingulate cortex to ultrasonic communicative vocalizations. *NeuroReport*, *28*(9), 479–484.

Smith, W. K. (1945). The functional significance of the rostral cingular cortex as revealed by its responses to electrical excitation. *Journal of Neurophysiology*, *8*(4), 241–255.

Sperli, F., Spinelli, L., Pollo, C., & Seeck, M. (2006). Contralateral smile and laughter, but no mirth, induced by electrical stimulation of the cingulate cortex. *Epilepsia*, *47*(2), 440–443.

Tschida, K., Michael, V., Takato, J., Han, B., Zhao, S., Sakurai, K., … Wang, F. (2018). Specialized neural circuit gates social vocalizations in the mouse. SSRN: 3249472.

Vertes, R. P. (2004). Differential projections of the infralimbic and prelimbic cortex in the rat. *Synapse (New York, N. Y.)*, *51*(1), 32–58.

Wöhr, M., & Schwarting, R. K. (2013). Affective communication in rodents: Ultrasonic vocalizations as a tool for research on emotion and motivation. *Cell and Tissue Research*, *354*(1), 81–97.

Yajima, Y., Hayashi, Y., & Yoshii, N. (1980). The midbrain central gray substance as a highly sensitive neural structure for the production of ultrasonic vocalization in the rat. *Brain Research*, *198*(2), 446–452.

Zhao, F., Jiang, H. F., Zeng, W. B., Shu, Y., Luo, M. H., & Duan, S. (2017). Anterograde trans-synaptic tagging mediated by adeno-associated virus. *Neuroscience Bulletin*, *33*(3), 348–350.

Zingg, B., Chou, X. L., Zhang, Z. G., Mesik, L., Liang, F., Tao, H. W., & Zhang, L. I. (2016). AAV-mediated anterograde transsynaptic tagging: Mapping corticocollicular input-defined neural pathways for defense behaviors. *Neuron*, *93*(1), 33–47.

**How to cite this article:** Bennett PJG, Maier E, Brecht M. Involvement of rat posterior prelimbic and cingulate area 2 in vocalization control. *Eur J Neurosci*. 2019;50:3164–3180. https://doi.org/10.1111/ejn.14477